

Modeling Tritium Behavior in Li_2ZrO_3 *

by

M. C. Billone
Energy Technology Division
Argonne National Laboratory
Argonne, IL 60436

RECEIVED
SER 16 88
OSTI

December 1997

The submitted manuscript has been authored
by a contractor of the U. S. Government
under contract No. W-31-109-ENG-38.
Accordingly, the U. S. Government retains a
nonexclusive, royalty-free license to publish
or reproduce the published form of this
contribution, or allow others to do so, for
U. S. Government purposes.

Presented at the Sixth International Workshop on Ceramic Breeder Blanket
Interactions (CBBI-6), October 22-23, 1997, Mito City, Japan. To be submitted
for publication in the proceedings of the meeting.

*Work supported by the United States Department of Energy, Office of Fusion
Energy Sciences, under Contract No. W-31-109-Eng-38

DISCLAIMER

This report was prepared as an account of work sponsored by an agency of the United States Government. Neither the United States Government nor any agency thereof, nor any of their employees, make any warranty, express or implied, or assumes any legal liability or responsibility for the accuracy, completeness, or usefulness of any information, apparatus, product, or process disclosed, or represents that its use would not infringe privately owned rights. Reference herein to any specific commercial product, process, or service by trade name, trademark, manufacturer, or otherwise does not necessarily constitute or imply its endorsement, recommendation, or favoring by the United States Government or any agency thereof. The views and opinions of authors expressed herein do not necessarily state or reflect those of the United States Government or any agency thereof.

DISCLAIMER

**Portions of this document may be illegible
in electronic image products. Images are
produced from the best available original
document.**

Modeling Tritium Behavior in Li_2ZrO_3 *

M. C. Billone

Energy Technology Division

Argonne National Laboratory

Abstract

Lithium metazirconate (Li_2ZrO_3) is a promising tritium breeder material for fusion reactors because of its excellent tritium release characteristics. In particular, for water-cooled breeding blankets (e.g., ITER), Li_2ZrO_3 is appealing from a design perspective because of its good tritium release at low operating temperatures. The steady-state and transient tritium release/retention database for Li_2ZrO_3 is reviewed, along with conventional diffusion and first-order surface desorption models which have been used to match the database. A first-order surface desorption model is recommended in the current work both for best-estimate and conservative (i.e., inventory upper-bound) predictions. Model parameters are determined and validated for both types of predictions, although emphasis is placed on conservative design predictions. The effects on tritium retention of ceramic microstructure, protium partial pressure in the purge gas and purge gas flow rate are discussed, along with other mechanisms for tritium retention which may not be dominant in the experiments, but may be important in blanket design analyses. The proposed tritium retention/release model can be incorporated into a transient thermal performance code to enable whole-blanket predictions of tritium retention/release during cyclic reactor operation. Parameters for the ITER driver breeding blanket are used to generate a numerical set of model predictions for steady-state operation.

*Work supported by the United States Department of Energy/Office of Fusion Energy, under Contract No. W-31-109-Eng-38.

1. INTRODUCTION

Lithium metazirconate (Li_2ZrO_3) is considered an attractive tritium breeding material for fusion reactor blankets because of its excellent tritium release properties, even at relatively low temperatures (e.g., $< 350^\circ\text{C}$). Several DEMO reactor designs^{1,2} and the ITER driver blanket design³ have specified the use of Li_2ZrO_3 in either sintered-product pellet form or pebble-bed form. The thermal and tritium performance properties of Li_2ZrO_3 and Li_2O have been compared by Billone in Ref. 4, along with approaches to modeling tritium transport in these two ceramic breeder materials.

The tritium retention/release database for Li_2ZrO_3 has undergone significant expansion during the past five years. The steady-state database comes from post-irradiation measurements of tritium inventory [I in weight parts per million (wppm)] in samples which have been irradiated in in-reactor purge-flow tests. Examples of such tests are the EXOTIC series (pebbles and pellets), BEATRIX-II Part II (pebbles), CRITIC-II (pebbles) and SIBELIUS (pellets). These data are generally normalized to the tritium generation rate (G in wppm/hour) to give a tritium residency time ($\tau = I/G$ in hours). The generation rate is taken from the last reactor cycle which is assumed to operate at a constant temperature profile and purge flow rate and composition for a time long enough to establish steady-state retention and release. Data from transient testing come from several methods: the difference between the transient release rate (R in wppm/hour) and the generation rate (G in wppm/hour) can be determined by integrating (G - R) in response to a sudden change in temperature or purge-protium-content to give the change in steady-state inventory (ΔI); the time-history of the release rate represents a detailed form of transient data; and the time-histories of the release data from post-irradiation isothermal anneal tests and/or temperature ramp tests represent a detailed form of transient data. In addition, data are also obtained from samples

irradiated at very low temperature and subjected to a post-irradiation isothermal anneal and/or temperature ramp tests. Finally, laboratory tests have been used to characterize the response of unirradiated Li_2ZrO_3 to moisture and hydrogen isotopes in the gaseous form.

In terms of models used to interpret tritium retention/release data, diffusion, first-order surface desorption and diffusion-desorption models are generally used, although surface adsorption and second-phase precipitation models are also included in more detailed treatments.^{5,6} The decision as to the degree of modeling sophistication required depends on the extent of the database and the application. MISTRAL⁵ is an example of a fundamental first-principles code for analyzing both transient and steady-state performance of ceramic breeders. However, several possible draw-backs to using MISTRAL as a design code are: a) the database is not extensive and thorough enough to allow determination and fine-tuning of the many pre-exponential constants and activation energies incorporated into the models; b) MISTRAL, which performs the analysis for a local radial slice of solid breeder, does not have the internal capacity to repeat this calculation many times to account for poloidal, toroidal and radial variations in operating conditions in order to generate a "whole-blanket" result; and c) it is difficult to incorporate and/or couple MISTRAL to a whole-blanket code which generates time- and space-dependent distributions of tritium generation rates and temperatures. TIARA⁶ is an example of a code with less-detailed, steady-state models for diffusion, first-order surface desorption, solubility and second-phase precipitation. Model parameters are determined from out-of-reactor testing of irradiated and unirradiated samples. Validation is performed by comparing code predictions to inventory data derived from post-irradiation data from samples which have been subjected to in-reactor purge-flow testing. However, several possible draw-backs to using TIARA as a design code are: a) to date, only model parameters for Li_2O have been determined and validated; b) the code is restricted in application to steady-state operation; and c) separate calculations must be performed for each radial

layer in a module and for each module in the poloidal direction with no internal means of integrating the results to obtain a whole-blanket result.

The objective of the current work is to generate a model for Li_2ZrO_3 tritium retention/release which reasonably matches, or at least bounds, the database, and yet is simple enough to incorporate into a whole-blanket code for design analysis of breeding blanket performance under steady and cyclic operation. Progress in model development is discussed in this current effort. Sample design calculations are presented for the case of the ITER driver blanket operating in a steady-state mode.

The effects on tritium retention of ceramic microstructure, protium partial pressure in the purge gas and purge gas flow rate are discussed, along with other mechanisms for tritium retention which may not be dominant in the experiments, but may be important in blanket design analyses. Additional test results, not included in the current work, are highlighted.

2. Diffusion vs. First Order Surface Desorption Models

Before the development of more sophisticated codes such as MISTRAL and TIARA, modeling of tritium behavior in lithium-based ceramics consisted of single mechanism (e.g., diffusion or desorption) or dual mechanism (e.g., diffusion and desorption) models. Both diffusion and first-order surface desorption models lead to the result that the steady-state tritium inventory [I in weight parts per million (wppm)] is linearly proportional to the tritium generation rate (G in wppm/hour) with the proportionality constant equal to the tritium residency time ($\tau = I/G$, where τ is commonly expressed in units of hours). For a single spherical grain, the diffusional residency time is related to the geometry of the sample according to

$$\tau = a^2/(15 D) \quad (1)$$

where a is the grain radius (in m) and D is the diffusion coefficient in m^2/hour . For the same geometry, the desorption residency time is related to the geometry of the sample according to

$$\tau = a/(3 k) \quad (2)$$

where k is the desorption rate constant. For each mechanism, there are two constants which can be determined by matching predictions to data:

$$D = D_0 \exp [-Q_{\text{dif}}/(R T)] \quad (3)$$

and

$$k = k_0 \exp [-Q_{\text{des}}/(R T)] \quad (4)$$

where D_0 and k_0 are pre-exponential constants, Q_{dif} and Q_{des} are effective activation energies for the respective mechanisms, R is the universal gas constant [8.314×10^{-3} kJ/(mol•K)] and T is the absolute temperature in K.

For porous, polycrystalline samples, it is customary to assume spherical grains and to use Eq. 1 for the diffusional tritium residency time. However, in the case of the desorption residency time, the volume to surface-area ratio term ($a/3$) in Eq. 2 is replaced by $(a_s \rho_{th})^{-1}$, where a_s is the specific pore-solid interface area (in m^2/g) for interconnected porosity and ρ_{th} is the theoretical density of the ceramic in g/m^3 . In addition, excess protium in the purge gas is assumed to enhance tritium release and to reduced tritium inventory. The adsorption of protium onto the surface of the ceramic is assumed to be proportional to the square root of the protium partial pressure[$(P_{H_2})^{0.5}$, where P_{H_2} is in Pa]. Thus, the surface desorption model predicts that the residency time for a porous solid purged by excess protium can be expressed as:

$$\tau = [a_s \rho_{th} k_o (P_{H_2})^{0.5}]^{-1} \exp [Q_{des}/(R T)] \quad (5)$$

Based on steady-state data alone, it is difficult to determine which mechanism is rate limiting unless the sample microstructure and the operating conditions are varied in a controlled manner. Both mechanisms result in a linear dependence of inventory on generation rate and an exponential increase in inventory as the temperature is lowered. However, for a spherical single crystal, the diffusion inventory increases as a^2 while the desorption inventory increases as a . Also, for samples purged by $He + H_2$, the diffusional inventory is independent of the protium content in the purge while the desorption inventory varies inversely as the square root of the protium partial pressure. It is more common to use porous, polycrystalline samples to study tritium behavior. This often results in a complication in the interpretation of the data. As the grain size is increased, the porosity tends to decrease and the pore-solid surface area tends to decrease, resulting in an increase in both diffusion and desorption inventory. Special fabrication procedures are required to increase the grain size at a constant pore-solid surface area. Furthermore, changes in the sample

microstructure and/or operating conditions during the in-reactor testing period may result in a change in the rate-limiting mechanism or a change into the transitional regime where both mechanisms are rate-limiting.

The mathematical solutions for transient diffusion vs. desorption appear to be quite different, but the numerical results are quite similar. Two examples are given in the following. In the first case, a spherical grain at uniform temperature T and zero initial tritium concentration experiences a step-function increase in generation rate from 0 to G . The release-rate fraction ($F_{rr} = R/G$) for a diffusion controlled mechanism is given by

$$F_{rr} = 1 - (6/\pi^2) \sum (1/n^2) \exp [-n^2 \pi^2 t/(15 \tau)] \quad (6)$$

where the sum in Eq. 6 is from 1 to ∞ and τ is defined by Eq. 1. For $F_{rr} < 0.2$ or $t/\tau < 0.015$, the short-time approximation to Eq. 6 may be used:

$$F_{rr} = 2.745874 (t/\tau)^{0.5} \quad (6a)$$

For longer times up to $F_{rr} = 0.95$ or $t/\tau = 5$, the intermediate-time solution to Eq. 6 may be used:

$$F_{rr} = 2.745874 (t/\tau)^{0.5} - 0.2 (t/\tau) \quad (6b)$$

The first-order desorption solution to the same problem is given by

$$F_{rr} = 1 - \exp(-t/\tau) \quad (7)$$

where τ is given by Eq. 2.

The two solutions (Eq. 6 and Eq. 7) are compared graphically in Fig. 1 for the same value of τ and, hence, the same steady-state inventory (time integration of G-R) and the same area under the fractional release rate curve. The diffusion solution initially rises more quickly from 0 to about 0.8 than does the desorption solution, but it approaches the steady-state solution of 1 more slowly. However, with experimental error in measuring tritium release, with generation rates that rise quickly (but not instantaneously) with time, and with temperature gradients generally associated with in-reactor test samples, the response time history is distorted and it is very difficult to determine diffusion-controlled release from desorption-controlled release based on the non-ideal, experimental release-rate history.

The second comparison example consists of the same spherical grain at the same steady generation rate. After steady-state release has been obtained, the temperature is increased instantaneously from T_1 to T_2 resulting in an increase in release rate fraction to above 1 and a decrease in steady-state inventory (ΔI). The corresponding decrease in residency time is from τ_1 to τ_2 , which implies an increase in diffusion coefficient if diffusion is rate-limiting or an increase in the desorption-rate constant if desorption is rate-limiting. The mathematical solution to this problem for the diffusion-rate-limiting case is

$$F_{rr} = 1 + (\tau_1/\tau_2 - 1)(6/\pi^2) \sum (1/n^2) \exp[-n^2 \pi^2 t/(15 \tau_2)] \quad (8)$$

The mathematical solution to this problem for the desorption-rate-limiting case is

$$F_{tr} = 1 + (\tau_1/\tau_2 - 1) \exp(-t/\tau_2) \quad (9)$$

The two solutions are compared in Fig. 2 to experimental data from EXOTIC-6 transient #E0121208, which involved an increase in average breeder temperature from 368°C to 468°C.⁷ In Ref. 7, based on a diffusion best-fit to the data, the residency times of $\tau_1 = 3.5$ hours and $\tau_2 = 0.28$ hours were determined. As shown in Fig. 2, using the same residency time value in the desorption model (Eq. 9) results in nearly identical results. With these residency times, both models give the same inventories at T_1 and T_2 , as well as the same inventory change (ΔI). Based on tritium measurement errors, on possible distortion of the tritium release time history as the signal travels long distances in purge tubes from sample to monitoring instrumentation, on the effects of temperature gradients through the sample and on the non-instantaneous nature of the temperature increase, it is, again, very difficult to distinguish mechanisms based on these transient results. Both models give a step change in release-rate fraction of 12.5 for the specified residency value times, while the data gives a peak change of only 5.5. Both models give approximately the same asymptotic return to steady-state.

In summary, diffusion, diffusion/desorption, and desorption models have been used to interpret tritium release data and to predict tritium behavior in blanket designs. In terms of steady-state results, the diffusion and desorption models give the same predictions when the same residency time values are used. The time-dependent predictions from the two models are too close to allow a

distinction in rate-limiting mechanism based on most available transient data sets for Li_2ZrO_3 . However, for other lithium-based ceramics, such as Li_2O , for which single-crystal lattice diffusivity has been measured, the calculated diffusion inventory is orders of magnitude lower than the inventory measured after in-reactor purge flow experiments.⁶ The surface desorption rate constant determined for Li_2O from very controlled tests gives much better agreement with measured tritium inventories than does the diffusion coefficient. Thus, within the solid breeder analytical and experimental communities, there is general agreement that surface desorption is more rate-limiting than diffusivity for the microstructures which have been extensively tested and are recommended for design application. In general, of course, these are fine-grained samples with grain diameters on the order of 1 μm .

In the current work, the desorption model is selected over the diffusion model for detailed evaluation and validation because there are stronger physical arguments for it being more rate-limiting than diffusion and because it is simpler to apply to design problems for which there are large temperature gradients and, in some cases such as ITER, cyclic operation.

3. Tritium Retention/Release Database

3.1 Steady-state database

Direct measurements of tritium inventory in Li_2ZrO_3 cylindrical-pellet and pebble samples have been made following in-reactor purge flow tests. Tables 1 and 2 summarize the pertinent microstructural parameters and operating conditions for samples irradiated in the EXOTIC 3-6 tests (pellets and pebbles),⁷ the BEATRIX-II Phase II test (pebbles),⁸ the CRITIC-II test (pebbles),⁹⁻¹¹

and the SIBELIUS test (pellets).¹² For the pellet data, the tritium inventories are quite low (≤ 0.1 wppm) for average breeder temperatures $\geq 390^{\circ}\text{C}$ and local temperatures $\geq 340^{\circ}\text{C}$. However, when scaled by the generation rate to give residency time, $\tau \leq 5.4$ hours under the same operating conditions. Figure 3 shows the variation in residency time for porous pellets with the volume averaged temperature. The variation in model parameters (e.g., grain size, pore-solid surface area, protium pressure) is not large enough and/or consistent enough to justify one model (e.g., surface desorption) over another (e.g., diffusion). These data do not scale very well with the square of the grain size, as would be suggested by a diffusion model. With the exception of the one SIBELIUS data point at 100 Pa protium pressure, the majority of the data are at the same protium pressure (300 Pa), making it difficult to justify surface desorption based on protium pressure. Normalizing the pore-solid surface area to $0.9 \text{ m}^2/\text{g}$, gives a variation of 0.44 to 1.67 in this surface-desorption parameter. The pore/solid surface area scaling gives results which have only marginally less scatter than the results with grain-size-squared scaling. For the most interesting case (EXOTIC-4, Capsule 16.1 with $\tau = 5.4$ hours), the pore-solid surface area is not given. Finally, it is difficult to determine an effective activation energy from Fig. 3, because of the insufficient number of data points, the scatter in the data points, and the temperature-gradient effects which are not included in the analysis. In principle, an upper-bound residency time correlation could be established for the given temperature regime, but there would be no confidence in assuming that the activation energy would be high enough to extrapolate the residency times to lower temperatures and still represent a lower bound.

The pebble bed data in Table 2 represent a large number of individual data points for individual pellets: 1 for EXOTIC-6, 38 for BEATRIX-II/Phase-II and 40 for CRITIC-II. However, there is a high degree of uncertainty in assigning a local temperature for each pebble and, hence, each data point. Table 2 summarizes the range of inventories measured for each region of the pebble bed and

the corresponding temperature range. The tritium residency times are plotted in Fig. 4 as a function of average sample temperature. The pebble grain sizes are about an order of magnitude higher than the pellet grain sizes. Specific pore/solid surface area is reported only for the CRITIC-II pebbles. The BEATRIX-II/Phase-II pebbles are expected to have a similar value. The 94% dense EXOTIC-6 pebbles are expected to have a significantly lower pore/solid surface area than the 80-85% dense pebbles for BEATRIX-II and CRITIC-II. If the results were normalized to a protium pressure of 300 Pa, then according to the surface desorption model the BEATRIX-II results would be multiplied by a factor of only 0.95 and the CRITIC-II results would be multiplied by a factor of 0.58. In general, tritium inventories are quite small (< 0.3 wppm) for $T \geq 400^\circ\text{C}$. Higher inventories are measured for the EXOTIC-II pebble bed (2.4 wppm at an average temperature of 360°C and local temperatures of 315 to 425°C) and the CRITIC-II pebble bed (6.3 ± 4.6 wppm at an average temperature of 285°C and a local temperature range of 170 to 400°C). While these pebble results are quite good for validating models for tritium retention/release, they are not adequate for distinguishing between diffusion and desorption models or for determining an effective activation energy.

3.2 In-reactor transient tritium release data

For the EXOTIC-5, EXOTIC-6 and CRITIC-II tests, a number of transient tritium release curves were recorded following a change in temperature or protium content in the purge gas. For BEATRIX-II, transient release data are available only for changes in protium content in the purge. In Ref. 7, the data for EXOTIC temperature transients are tabulated in terms of the diffusional residency times which gave either the best fit to the inventory change (ΔI) and/or the time dependent release. The $\Delta\tau = \Delta I/G$ values are determined by integrating over time the transient release rate (R) minus the generation rate (G). The determination of $\Delta\tau$ in this manner results in values which are independent of models and, hence, can be used to determine model parameters

for either a diffusion or a desorption model. The major uncertainty in this approach is associated with the long periods of time for which the final release rate is close, but not equal, to the generation rate. Following temperature increases, the release rate seems to come to a steady-state value which is slightly above the generation rate. The opposite occurs following a temperature decrease in that the apparent steady-state release rate is slightly below the generation rate. However, in the detailed tables in Ref. 7, it is not clear which residency times were determined by this method. It appears that most of the residency times in Ref. 7 were determined as values of τ which give a best-fit of the diffusion model to the measured transient release rate data vs. time. As shown in Fig. 2, a surface desorption approach would have led to essentially the same values of tritium residency time.

The values of residency time reported in Ref. 7 based on temperature-change data are shown in Fig. 5 (pellet data) and Fig. 6 (pebble-bed data) vs. the inverse of the average temperature in K. The scatter in the data is more than an order of magnitude for the pellet data (more samples with different microstructures) and less than an order of magnitude for the pebble data.

3.3 Transient data from postirradiation isothermal anneals and/or temperature ramps

In addition to the data described in the two previous subsections, data are also available in the literature for samples irradiated at low temperature and subjected to laboratory postirradiation isothermal annealing and or linear temperature ramp testing. Uncertainties associated with these data sets are: possible release of some of the tritium during irradiation; spatial distribution of tritium following irradiation, level of tritium remaining in the samples after testing. These data have not yet been used to validate the proposed surface desorption model.

4. Determination of Parameters for the First-Order Surface Desorption Model

4.1 Transient data for Li_2ZrO_3 EXOTIC-5,6 pellets

The motivation for separating the residency time data for cylindrical pellets (Fig. 5) from the residency time for pebble beds (Fig. 6) is the large difference in microstructures (grain sizes and specific pore/solid surface area) for the two types of samples. Both the larger grain size and the implicitly smaller pore/solid surface area of the pebble beds suggest that inventories and residency times should be higher for the pebbles. However, even with this separation of databases, the scatter in the data is too large to allow model parameters to be selected with confidence.

The authors of Ref. 7 suggest ways to filter and group the data. Residency times determined from the first reactor cycle (approximately 25 days) tended to be smaller than residency times determined from subsequent cycles. Residency times determined from temperature decrease transients tended to be smaller than residency times determined from temperature increase experiments. For design application, the main interest is in long-time behavior. For ITER application the long-time behavior at low temperature is of particular interest.

In Fig. 5, the pellet residency times have been determined from temperature increase and temperature decrease experiments at reference purge flow conditions ($\text{He}+0.1\%\text{H}_2$, 0.3 MPa pressure, 100 ml/minute flow rate). The results of the first 25-day cycle of operation have been omitted from this plot. Also, the data are separated into temperature increase and temperature decrease values. While, for a specific sample, it may be true that temperature rise experiments lead to higher values of residency time than do temperature decrease experiments, the scatter of results from sample to sample appears to be greater than this effect for any one sample. Best fit correlations to the values of residency time data are:

$$\text{Temperature rise experiments: } \tau = \exp(-12.569 + 8.309 \times 10^3/T), \text{ hours} \quad (10a)$$

Average of all data: $\tau = \exp(-12.068 + 7.911 \times 10^3/T)$, hours (10b)

Temperature decrease experiments: $\tau = \exp(-11.577 + 7.536 \times 10^3/T)$, hours (10c)

Because the scatter is so large for the residency times of these samples and the effective activation energies are relatively close (69 kJ/mole for Eq. 10a, 66 kJ/mole for Eq. 10b, and 63 kJ/mole for Eq. 10c), it is recommended that the best-fit correlation to all of the data (Eq. 10b) be used as a first estimate of the tritium residency time for pellets with microstructures and purge conditions within the range of those for EXOTIC-5 through -6 samples.

4.2 Transient data Li_2ZrO_3 EXOTIC-6 pebbles

In Fig. 6, tritium residency times are shown for temperature rise and temperature decrease experiments for the EXOTIC-6 Li_2ZrO_3 pebble bed. As expected, there is less scatter in the results, because all of the data come from the single pebble bed, whereas the pellet data came from samples with different microstructures. The data from the first reactor cycle have been omitted from this data set. The best-fit correlations to the temperature rise data (1), all the data (2) and the temperature decrease data (3) are:

Temperature rise experiments: $\tau = \exp(-18.7916 + 1.3291 \times 10^4/T)$, hours (11a)

Average of all data: $\tau = \exp(-15.328 + 1.1033 \times 10^4/T)$, hours (11b)

Temperature decrease experiments: $\tau = \exp(-13.237 + 9.609 \times 10^3/T)$, hours (11c)

4.3 Best-estimate and upper-bound correlations for pellets

It is assumed that the effective activation energy derived from the transient data is representative of the rate-limiting surface-desorption mechanism. The directly-measured tritium inventory data (normalized to the generation rate to give residency time) are used to determine the pre-exponential factor for best-fit and upper-bound correlations. Figure 7 shows the results of this exercise for the cylindrical pellets used in EXOTIC-3,4,5,6 and SIBELIUS. The SIBELIUS data point has been normalized to the EXOTIC protium level of 300 Pa, by assuming that the residency time for surface desorption varies inversely with the square root of the protium pressure for protium/tritium ratios $\gg 1$. Eleven data points are shown in Fig. 7. Only ten are used in the analysis. The EXOTIC-3 residency time of 0.75 hours at an average temperature of 630°C appears to be unreasonable. The best fit correlation (τ_{bf} in hours) to the steady-state data is

$$\tau_{bf} = (300 \text{ Pa}/P_{H_2})^{0.5} \exp(-12.222 + 7.911 \times 10^3/T) \quad (12)$$

The “reasonable” upper bound correlation (τ_{ub} in hours) is derived by matching the four highest residency times at a given temperature (see Tables 1 and 2): 2.4 hours for EXOTIC-3 sample at an average temperature of 405°C, 4.6 hours for EXOTIC-4 sample at an average temperature of 410°C, 5.4 hours for EXOTIC-4 sample at an average temperature of 360°C, and 0.34 hours scaled to 0.20 hours for SIBELIUS sample at an average temperature of 545°C. The results are:

$$\tau_{ub} = (300 \text{ Pa}/P_{H_2})^{0.5} \exp(-10.644 + 7.911 \times 10^3/T) \quad (13)$$

The results from Eqs. 12 and 13 are shown in Fig. 7.

4.4 Best-estimate and upper-bound correlations for pebbles

The data in Fig. 4 have been normalized to a protium pressure of 300 Pa and reploted in Fig. 8. For the BEATRIX-II data, the residency times have been scaled by $(270/300)^{0.5} = 0.95$, which is a small correction. The CRITIC-II data have been scaled by $(100/300)^{0.5} = 0.577$. Although the CRITIC and BEATRIX data sets represent inventory measurements from a large number of pebbles, it is difficult to use the data for model improvement and validation because of the uncertainties in the temperature of each pebble. The horizontal lines in Fig. 8 represent the range of temperatures in the region in which the pebbles were selected. These ranges are quite large for BEATRIX and CRITIC samples. The vertical lines represent the average value and standard deviation of the data. However, plotting the average value vs. the average temperature is misleading. All of the pebbles within the temperature region would have to be measured in order to get a true average. This is particularly true of the CRITIC-II outer ring pebbles for which inventory values varied considerably. It is less important for the hotter inner rings ($T > 400^\circ\text{C}$) where inventories are quite low. The EXOTIC-6 data point in Fig. 8 is a true average value because the tritium in the whole sample was measured. Thus, it has a higher weighting value for correlation refinement and validation than do the low temperature CRITIC-II data.

Given the large uncertainties involved in interpreting the inventory data for pebbles, it was not possible to determine a best-fit and an upper-bound correlation for residency time. In considering tritium residency time correlations (Eq. 11a-c) determined from transient EXOTIC-6 data, it was observed that Eq. 11a is very consistent with the residency time derived from the post-irradiation measurement. Thus, with only a small modification, it is recommended for design calculations. For temperatures below $\approx 400^\circ\text{C}$, the correlation is believed to give an upper bound on the tritium residency time. This observation is certainly true for the CRITIC-II data from the $170\text{-}400^\circ\text{C}$

region of the bed. For temperatures above $\approx 560^{\circ}\text{C}$, the correlation is a lower bound of the data. Thus, the correlation is arbitrarily limited to a residency time of 0.1 hours for $T > 560^{\circ}\text{C}$.

$$\tau_{ub} = (300 \text{ Pa}/P_{H2})^{0.5} \exp(-18.259 + 1.329 \times 10^4/T) \text{ for } T \leq 833 \text{ K} \quad (14a)$$

and

$$\tau_{ub} = 0.1 (300 \text{ Pa}/P_{H2})^{0.5} \text{ for } T > 833 \text{ K} \quad (14b)$$

5. Design Application

Equations 12, 13 and 14 are used to calculate best-estimates and upper-bound estimates for the Li_2ZrO_3 breeder layers of the lowest-breeder-temperature ITER design described by Y. Gohar in Ref. 12. Table 3 gives the masses, tritium generation rate, minimum/maximum temperature, and calculated inventory for each layer, as well as the total. Calculations were performed by integrating the product of the generation rate and residency time, with the spatial variations in temperature and generation rate included in the calculation. The sintered product design is assumed to consist of fine-grained ($\sim 1 \mu\text{m}$), low density ($\sim 70\%$) Li_2ZrO_3 cubes. The pebble bed design is assumed to consist of coarse grained ($10\text{-}40 \mu\text{m}$), high density ($\sim 94\%$) large pebbles with diameter of 0.5 mm (e.g., EXOTIC-6 pebbles) packed to $\sim 60\%$ packing fraction and smaller diameter pebbles with the same microstructure packed to about $\sim 14\%$ packing fraction.

The best-estimate of the tritium inventory in the sintered-product pellet design (SPBE) is only 12 g, even with a minimum temperature of 267°C . The upper-bound estimate for the sintered-product pellet design (SPUB) is 58 g, which is still reasonable from a design perspective. The pebble-bed upper-bound (PBUB) actually only applies to the EXOTIC-6 pebble microstructure and not to

Li_2ZrO_3 pebble beds in general. The estimated inventory of 280 g is considered a significant amount by design standards. Most of the inventory is concentrated in the third layer (farthest from the plasma) of design configuration #3 which has the lowest values of T_{\min}/T_{\max} . Using data from BEATRIX-II/Phase-II and CRITIC-II type pebbles with smaller grain sizes (5-10 μm) and densities (80-85%) would lead to lower calculated inventories for the pebble bed design.

A major uncertainty in using the residency time approach to extrapolate to design conditions is the effect of the reduced protium-to-tritium ratio in the design. The data base for the correlations involves over-purged systems with protium-to-tritium ratios ranging from ~70 (CRITIC-II, end-of-life) to ~2200 (EXOTIC-4, Capsule 16.1). Currently, the proposed surface-desorption model considers the ratio of tritium to the square-root of the protium pressure in determining the tritium inventory. It remains to be demonstrated what minimum value of protium-to-tritium ratio is required in order for this model to be valid.

6. Discussion

The present work represents a first attempt to develop a simple model to be used in the extrapolation of transient and steady-state tritium release/retention data to design applications. The next stages in the model development involve:

- a. normalizing the data to specific surface area -- used to determine the ratio of interconnected pore surface area to solid volume -- as well as to the square-root of the protium pressure;
- b. exploring methods for reducing the scatter in the determination of residency time from the EXOTIC-5&6 transient data; Currently, some scatter reduction was achieved by eliminating data from the first 25 days of irradiation and separating the data into temperature rise

vs. temperature decrease data. In the process of doing this, it has been observed that using only the residency times determined for the final temperature of a temperature change reduce the scatter significantly. There is certainly analytical justification for doing this;

- c. exploring two-mechanism diffusion/desorption models to rationalize the difference in apparent activation energies between fine-grained/low-density pellets (66 kJ/mol) and large-grain/high-density pebbles (111 kJ/mol);
- d. fine tuning the model parameters and validating the model by using it to integrate over the temperature distribution of the sample and comparing predicted inventory to measured inventory;
- e. incorporating the laboratory data for tritium release during postirradiation annealing of the samples;
- f. using laboratory data on surface adsorption/desorption and solubility of moisture and gaseous hydrogen isotopes to explore slower mechanisms of tritium retention/release than those observed in the over-purged, in-reactor experiments (e.g., see Ref. 14)
- g. continue to test modeling assumptions and refine model parameters against data which are forthcoming (e.g., EXOTIC-7&8)

7. Conclusions

Progress in modeling the tritium retention/release behavior of Li_2ZrO_3 sintered-product pellets and pebbles has been reported. A surface desorption model, which includes the effects of specific

surface area and protium pressure in the purge -- has been proposed and tested against available in-reactor tritium release data and post-irradiation measurements of tritium inventory. Transient, on-line data from the EXOTIC-5&6 experiments on low-density, fine-grained Li_2ZrO_3 cylindrical pellets have been used to determine an effective activation energy (66 kJ/mol) for surface desorption. The pre-exponential factor in the model has been adjusted to achieve both best-fit and upper-bound model parameters for extrapolation of data to blanket designs such as ITER. A similar approach was used to derive an upper-bound surface desorption effective energy (111 kJ/mol) and pre-exponential factor for the high-density, large-grain-size pebbles tested in the EXOTIC-6 experiments. The models were applied to the design conditions for a candidate ITER driver blanket to predict the distribution of tritium inventory in such a blanket design. Recommendations are made on how to improve the modeling effort by including more data sets and more sophisticated models.

References

1. N. Roux, J. Mouglin, B. Rasneur, E. Proust, L. Giancarli and J. F. Salavy, "Current Material and Design Studies in View of the Utilization of Li_2ZrO_3 in the BIT Blanket Concept," *J. Nucl. Mater.*, 212-215 (1994) 862-867.
2. P. Lorenzetto, P. Gierszewski, S. Chiocchio, G. Federici, H. Gorenflo, M. Iseli, H. McIlwain, E. Salpietro and G. Williams, "A Driver Blanket for NET," *Proc. 17th Symp. Fus. Tech. (SOFT-17)*, Rome, Sept. 14-18, 1992, 1414-1418.
3. Y. Gohar, M. Billone, A. Cardella, W. Dänner, K. Ioki, T. Kuroda, D. Lousteau, P. Lorenzetto, S. Majumdar, R. Mattas, R. Raffray, Y. Strebkov, H. Takatsu and E. Zolti, "ITER Breeding Blanket Design," *Proc. Symp. Fus. Eng. (SOFE 95)*, Sept. 30-Oct. 5, 1995, pp. 410-417.

4. M. C. Billone, "Thermal and Tritium Transport in Li_2O and Li_2ZrO_3 ," *J. Nucl. Mater.* 233-237 (1996) 1462-1466.
5. A. R. Raffray, M. C. Billone, G. Federici and S. Tanaka, "Progress in Tritium Retention and Release Modeling for Ceramic Breeders," *Fus. Eng. Des.*, 28 (1995) 240-251.
6. M. C. Billone, "TIARA Analysis of Tritium Inventory in Li_2O ," *Fus. Eng. Des.* 28 (1995) 313-318.
7. H. Kwast, M. Stijel, R. Muis and R. Conrad, "EXOTIC: Development of Ceramic Tritium Breeding Materials for Fusion Reactor Blankets, The Behaviour of Tritium in: Lithium Aluminate, Lithium Oxide, Lithium Silicates, and Lithium Zirconates," Petten Report ECN-C-95-123, December, 1995.
8. O. D. Slagle and G. W. Hollenberg, "BEATRIX-II, Phase II: Data Summary Report," Pacific Northwest National Laboratory, Report No. PNNL-11148, May 1996.

9. J. M. Miller and R. A. Verrall, "Performance of a Li_2ZrO_3 Sphere-Pac Assembly in the CRITIC-II Irradiation Experiment," *J. Nucl. Mater.* 212-215 (1994) 897-901.
10. R. A. Verrall, J. M. Miller and L. K. Jones, "The CRITIC-II On-Line Irradiation of Lithium Zirconate Pebbles," Proc. Fifth International Workshop on Ceramic Breeder Blanket Interactions (CBBI-5), Rome, Sept. 23-25, 1996, ed. S. Casadio (ENEA), pp 117-129.
11. R. A. Verrall, J. M. Miller and L. K. Jones, "The CRITIC-II On-Line Irradiation of Lithium Zirconate Pebbles," AECL-11768, CFFTP-9637, March 1997.
12. J. P. Kopasz and C. E. Johnson, "Performance of Ceramic Breeder Materials in the SIBELIUS Experiment," *J. Nucl. Mater.* 219 (1995) 259
13. Y. Gohar, ITER/JCT-Garching, personal communication, Oct. 2, 1997
(material presented at the ITER Blanket Meeting, San Diego, Oct. 2-4, 1997)

14. C. Alvani, P.L. Carconi, M. R. Mancini, A. Moauro, F. Pierdominici, A. Masci and S. Casadio, "Purge Gas Interactions with Ceramic Breeder Pebbles," Sub-TASK B3-2.1 -- 1996 Activity Report, ENEA Document INN/NUMA/MATAV(97)1

Table 1. Summary of microstructure, operating conditions and measured tritium inventory following irradiation in EXOTIC-3, 4 and 5 in-reactor purge flow tests. Numbers in parentheses below the experiment number are the capsule number. All samples are solid or hollow cylindrical pellets. Operating conditions apply to last reactor cycle prior to shut-down.

Parameter	EX-3 (11.1)	EX-3 (12.1)	EX-4 (14.1)	EX-4 (14.2)	EX-4 (16.1)	EX-5 (17.1)	EX-5 (21.1)	EX-5 (18.1)
Mass, g	35.75	35.75	59.4	58.9	34.6	21.3	20.0	16.0
Density, %td	79	79	86	85	79	77.5	74.5	74
Open Porosity, %	20	20	14	15	21	19.5	25.5	26
Pore-Solid Surface Area, m ² /g	0.4	0.4	0.9	0.9	---	0.9	0.9	1.2
Grain Diam., μm	2.5	2.5	1.0	1.0	0.7	0.9	0.8	1.1
Protium Partial Pressure, Pa	300	300	300	300	300	300	300	300
Generation Rate, wppm/hour	0.0227	0.0241	0.0158	0.0191	0.0209	0.130	0.144	0.137
Temperature, °C	650	425	460	680	380	460	480	410
Inner	630	405	410	635	360	430	450	390
Average	610	385	360	590	340	400	420	370
Outer								
Li Burnup, at.%	0.1	0.1	0.13	0.13	0.13	1.8	2.05	1.9
Inventory, wppm	0.018	0.06	0.075	0.001	0.117	0.007	0.009	0.1
Residency Time, hours	0.75	2.4	4.6	0.05	5.4	0.05	0.06	0.73

Table 2. Summary of microstructure, operating conditions and measured tritium inventory following irradiation in EXOTIC-6, BEATRIX II (Phase II), CRITIC-II, and SIBELIUS in-reactor purge flow tests. All samples are solid or hollow cylindrical pellets. Operating conditions apply to last reactor cycle prior to shut-down.

Parameter	EX-6 (21.1)	EX-6 (21.2)	SIB.	EX-6 (24.2)	BEAT.-II Phase-II	CRITIC-II
Sample Form	Pellet	Pellet	Pellet	Pebble Bed	Pebble Bed	Pebble Bed
Mass, g	9.22	10.58	1.00	8.16	29.5	203
Density, %td	73	81	81	94 (peb) 52.5 (bed)	80-82 (peb) 53 (bed)	80-85 (peb) 53 (bed)
Open Porosity, %	27	19	19.5	6 (peb)	14-16 (peb)	14-16 (peb)
Pore-Solid Surface Area, m^2/g	1.5	0.8	---	---	(0.34 ± 0.12)	0.34 ± 0.12
Grain Diam., μm	1	2	1	10-40	10	5-10
Protium Partial Pressure, Pa	300	300	100	300	270	100
Generation Rate, wppm/hour	0.252	0.227	0.064	0.27	0.443	0.026
Temperature, $^{\circ}\text{C}$						
Inner	485	495	550	425	985	900
Average	450	455	545	360	---	---
Outer	440	445	540	315	395	170
Li Burnup, at.%	3.01	3.02	0.8	3.11	3.1	0.5
Inventory, wppm	0.009	0.015	0.022	2.4	0.32 ± 0.01 (395-770 $^{\circ}\text{C}$) 0.15 ± 0.12 (770-945 $^{\circ}\text{C}$) 0.032 ± 0.01 (945-1025 $^{\circ}\text{C}$)	6.3 ± 4.6 (170-400 $^{\circ}\text{C}$) 0.009 ± 0.009 (400-750 $^{\circ}\text{C}$) 0.002 ± 0.002 (750-900 $^{\circ}\text{C}$)
Residency Time, hours	0.04	0.07	0.341	9.5	0.72 ± 0.02 (395-770 $^{\circ}\text{C}$) 0.34 ± 0.27 (770-945 $^{\circ}\text{C}$) 0.072 ± 0.023 (945-1025 $^{\circ}\text{C}$)	244 ± 178 (170-400 $^{\circ}\text{C}$) 0.4 ± 0.5 (400-750 $^{\circ}\text{C}$) 0.078 ± 0.116 (750-900 $^{\circ}\text{C}$)

Table 3. Summary of ITER Driver Blanket Design A Parameters for 100% Dense Beryllium Layers and 70% Dense Solid Breeder (Li_2ZrO_3) Layers. The design consists of 24 breeding modules in the poloidal direction. The inventory calculations are for sintered-product-best-estimate (SPBE) correlation, sintered-product-upper-bound (SPUB) correlation and pebble-bed-upper-bound (PBUB) correlation. The purge is assumed to be He at atmospheric pressure (0.1 MPa) with 0.1% H_2 and a flow rate giving a protium-to-tritium ratio > 10 locally and ~ 20 on the average.

Config./ Layer	Mass MT	Generation Rate, g/day	T_{\min}/T_{\max} °C	I(SPBE) g	I(SPUB) g	I(PBUB) g
3/1	15.559	75.396	425/764	0.4	2.1	1.6
3/2	23.338	56.995	313/667	2.4	11.4	31.3
3/3	23.338	23.291	267/417	5.5	26.5	169
2/1	5.386	16.010	357/785	0.2	1.1	1.5
2/2	5.386	11.254	297/564	0.8	3.9	13.8
1/1	5.574	24.584	338/605	0.6	3.1	5.6
1/2	8.360	18.772	271/550	2.1	10.2	56.8
Total	87	226	267/785	12	58	280

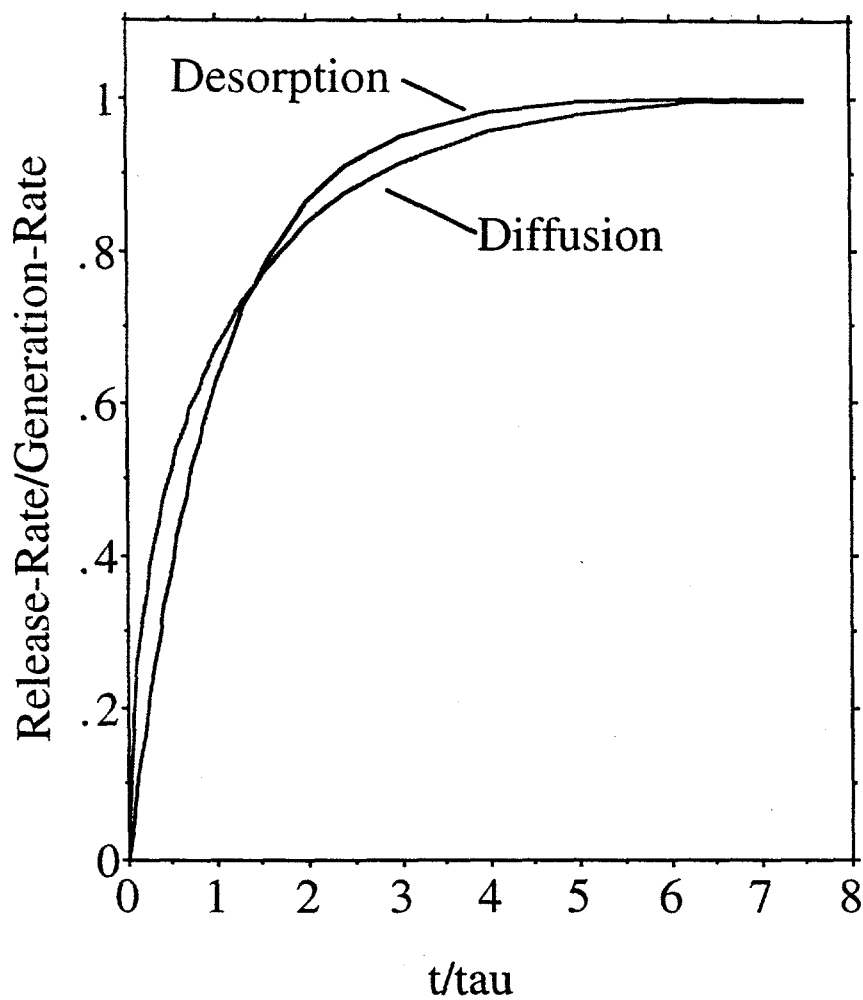


Fig. 1. Comparison of analytical solutions for first-order surface desorption and bulk diffusion for an isothermal spherical grain in response to an instantaneous increase in generation rate at time $t = 0$. Tau is the residency time and is equal to the steady-state inventory (I) divided by the generation rate (G): $\tau = I/G$. Both models have the same steady-state inventory, but slightly different time dependence.

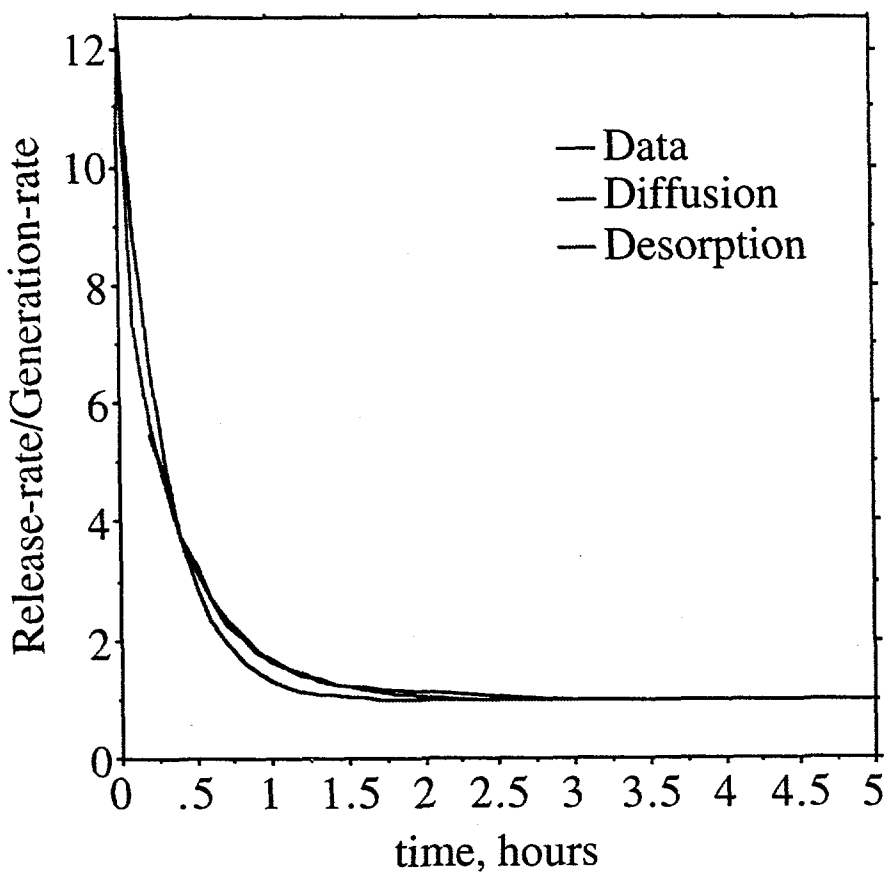


Fig. 2. Comparison of diffusion and desorption model predictions to the tritium release rate data (normalized to the generation rate) vs. time for the EXOTIC-6 transient E0121208 for Li_2ZrO_3 capsule 21.2 exposed to an increase in average temperature from 368°C to 468°C . Both models use the same tritium residency time and give the same long-time decrease in tritium inventory. The diffusion model prediction is essentially coincident with the data after 0.2 hours when the data are shifted by 0.2 hours. The desorption model predictions also give good agreement with the data.

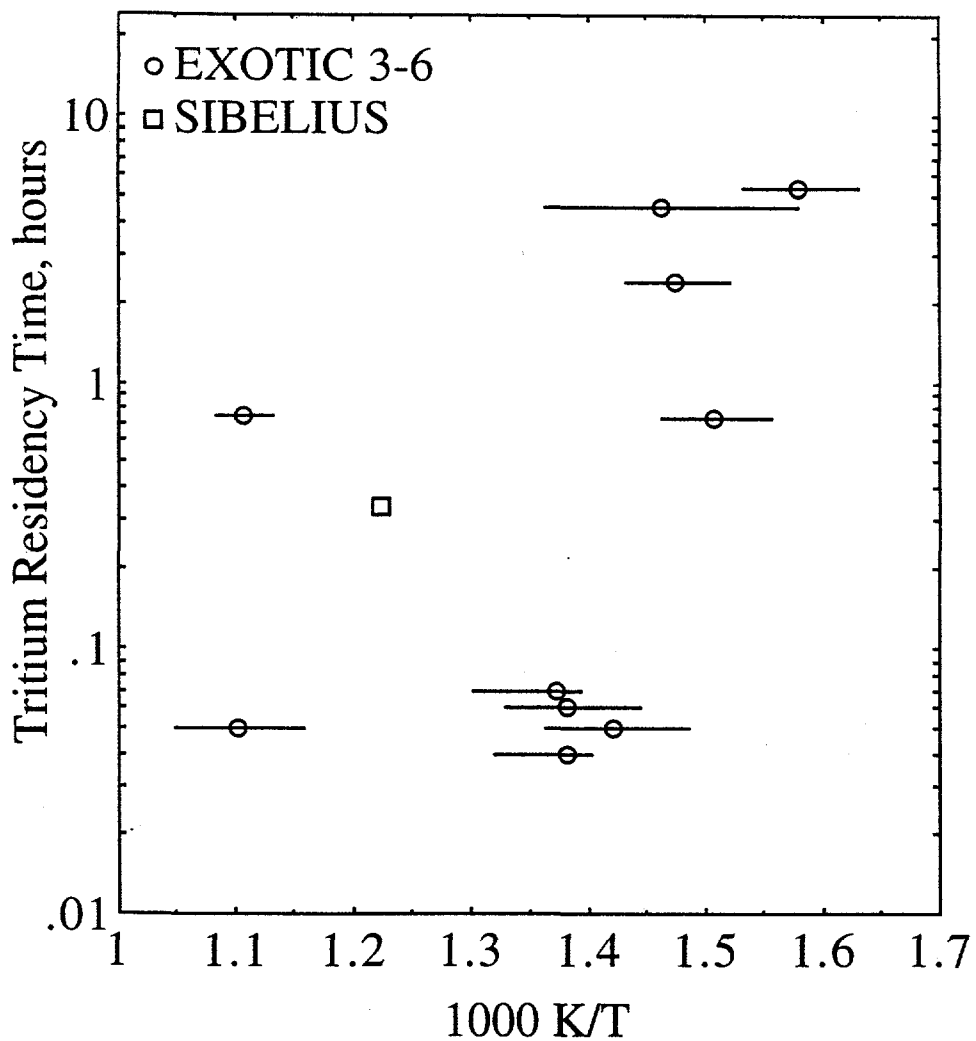


Fig. 3. Tritium residency time derived from EXOTIC-3 to -6 and SIBELIUS Li_2ZrO_3 cylindrical-pellet inventory data. The residency time is determined from postirradiation inventory data divided by the generation rate during the last cycle of irradiation. The average pellet temperature is used to derive $1000 \text{ K}/T$, where T is in K. Grain sizes range and densities range from 0.7 to 2.5 μm and 73-86%, respectively. The horizontal bands show the range of temperature from T_{\min} to T_{\max} for each sample. Temperature range is 315-680°C.

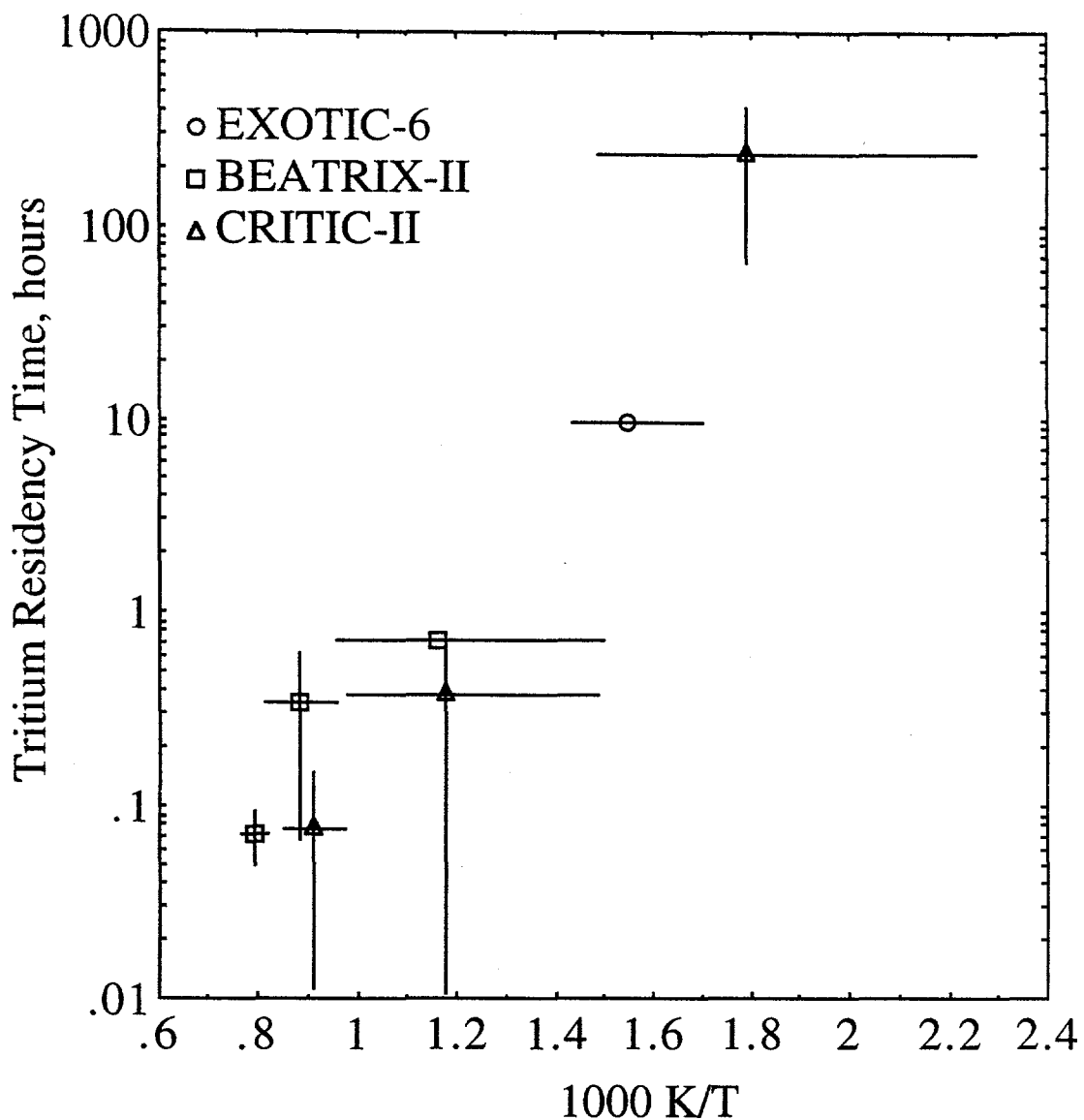


Fig. 4. Tritium residency time derived from EXOTIC-6, BEATRIX-II/Phase-II and CRITIC-II Li_2ZrO_3 pebble-bed inventory data. The residency time is determined from postirradiation inventory data divided by the generation rate during the last cycle. The average pebble-bed-region temperature is used to derive $1000 \text{ K}/T$, where T is in K. The horizontal lines show the temperature range for the pebbles examined. The vertical lines show the one-standard-deviation of the measurements. Temperature range is 170-1025°C.

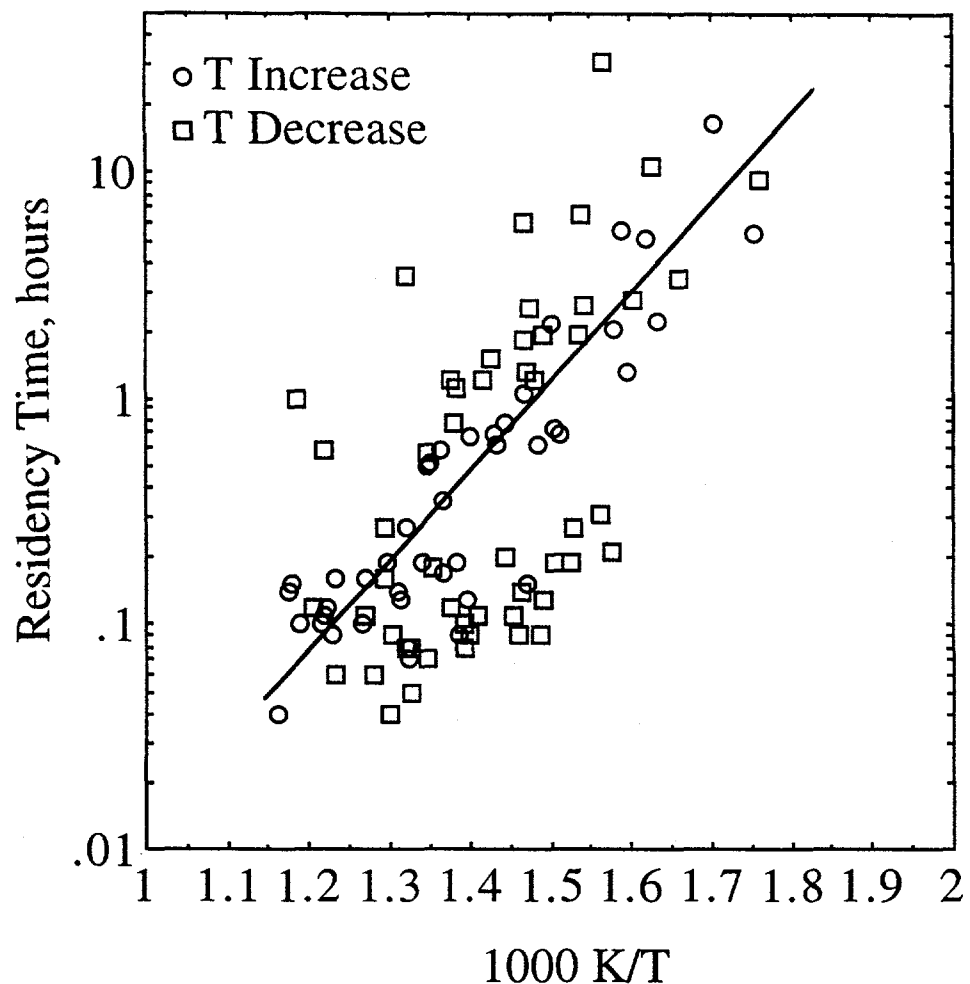


Fig. 5. Tritium residency time vs. the inverse of the average temperature (in K) for sintered-pellet Li_2ZrO_3 based on on-line EXOTIC-5 and EXOTIC-6 tritium release data in response to temperature transients. Pellet densities range from 73 to 81% of theoretical, grain sizes range from 0.8 to 2.0 μm and Li burnups range from 1.8 to 3.0 at.%. All tests were conducted in He + 0.1 vol.% H_2 purge at 100 ml/minute and 0.3 MPa. The line represents the best-fit correlation to the transient data for pellets: $\tau = \exp(-12.0684 + 7.911 \times 10^3/T)$, hours.

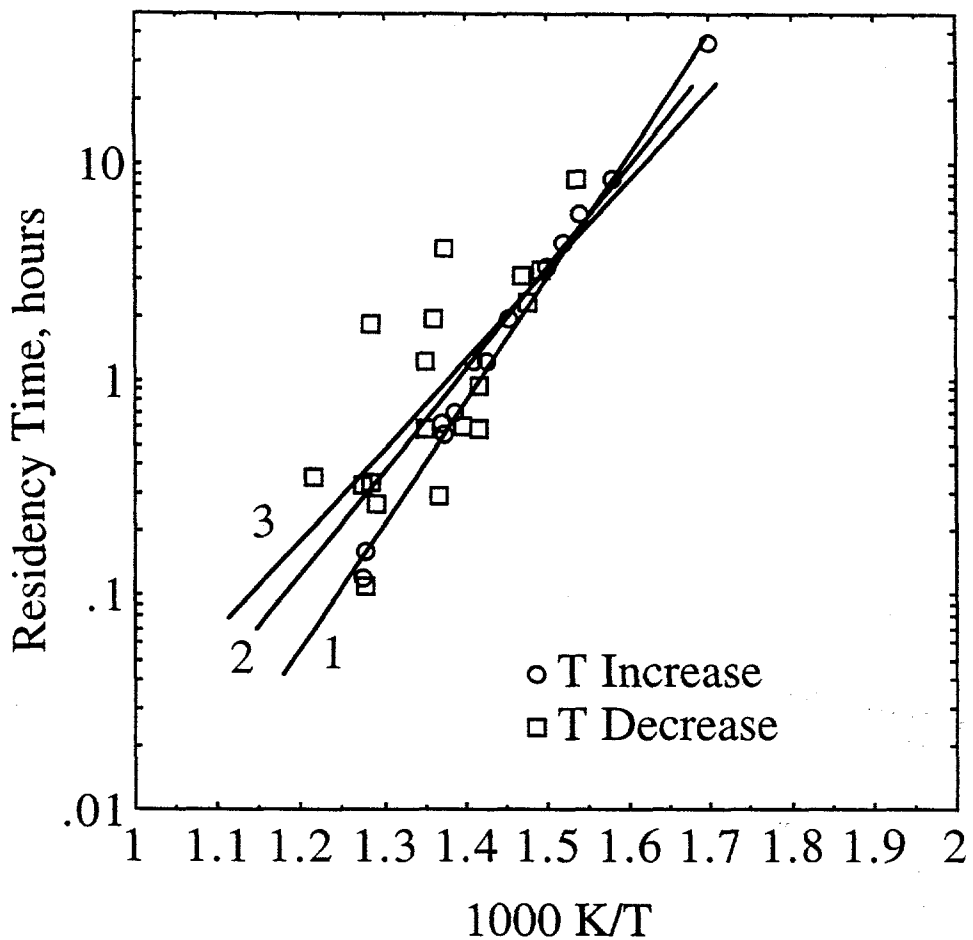


Fig. 6. Tritium residency time vs. the inverse of the average temperature (in K) for the EXOTIC-6 Li_2ZrO_3 pebble bed, based on on-line tritium release data in response to temperature transients. The 0.5-mm pebbles are 94% dense with 10-40 μm grain size and smear density of 52.5%. All tests were conducted in He + 0.1 vol.% H_2 purge at 100 ml/minute and 0.3 MPa. The residency time correlations for the temperature increase data (1), the average of the data (2), and the temperature decrease data (3) are: 1. $\tau = \exp(-18.7916 + 1.3291 \times 10^4/T)$ hours, 2. $\tau = \exp(-15.3278 + 1.1033 \times 10^4/T)$ hours and 3. $\tau = \exp(-13.2369 + 9.609 \times 10^3/T)$ hours.

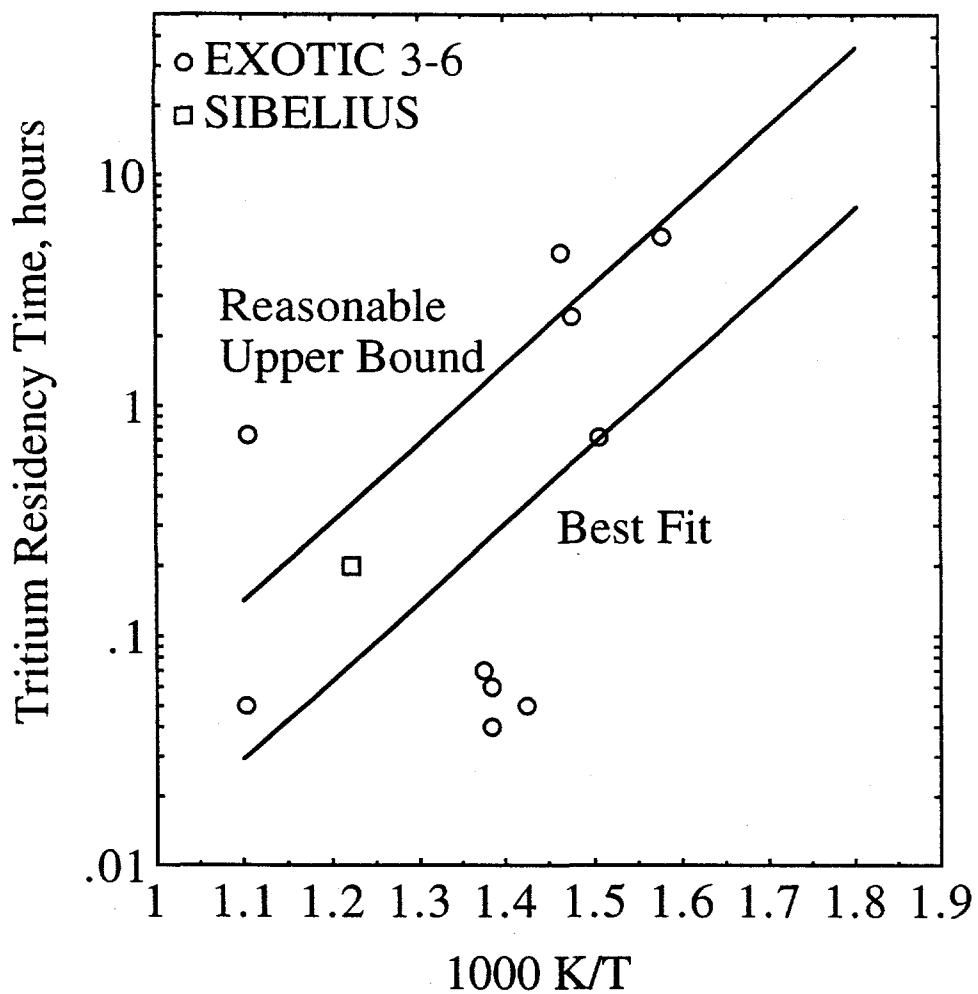


Fig. 7. Best-fit and reasonable upper bound correlations for Li_2ZrO_3 pellet residency time based on the EXOTIC-3,4,5,6 and SIBELIUS inventory measured directly (after irradiation) divided by the generation rate during the last reactor cycle. The activation energy is pre-determined from the EXOTIC-5,6 transient data. The pre-exponential for the best fit correlation is based on an average of 10 of the data points (EXOTIC-3 residency time of 0.75 hours at an average breeder temperature of 630°C excluded). The pre-exponential for the "reasonable" upper bound is based on matching the highest inventory data within a given temperature range. Pellet density and grain diameter ranges are 73-86% and 0.7-2.5 μm , respectively. The SIBELIUS data point has been normalized from 100 to 300 Pa of purge H_2 by dividing by $(3)^{0.5}$. Purge flow rate is the standard 100 ml/min.

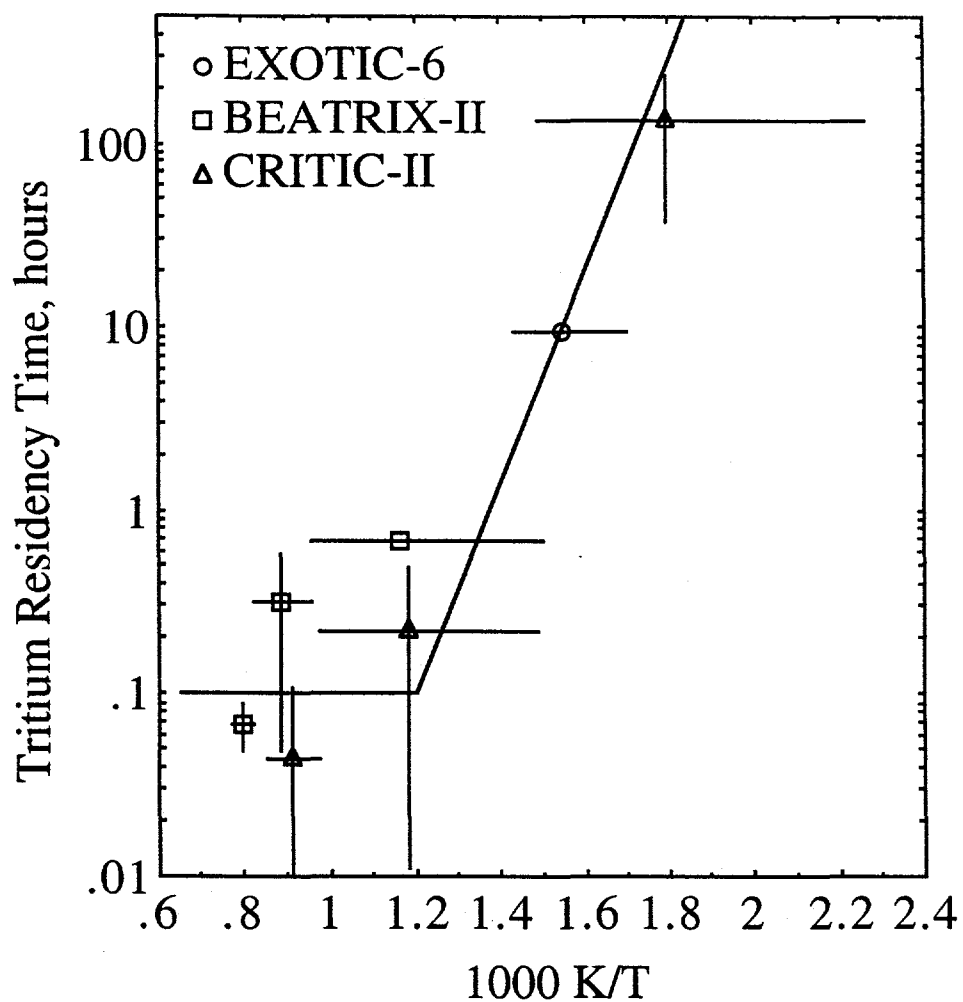


Fig. 8. Comparison of recommended upper bound correlation for pebble-bed Li_2ZrO_3 tritium residency time with pebble-bed data from EXOTIC-6, BEATRIX-II and CRITIC-II experiments. Experimental residency time is derived from the ratio of the measured tritium inventory after the irradiation divided by the generation rate during the last test cycle. All results have been normalized to the EXOTIC-II protium pressure (300 Pa) by assuming that the inventory is inversely proportional to the square root of the protium pressure. The data set includes pebble densities of 80-94%, grain diameters of 5-40 μm , pebble diameters of 0.5-2 mm and smear densities $\approx 53\%$. The purge flow rate is 100 ml/minute for all test data.